Geochemical Perspectives Letters EAG

Consolidating the isotopic trichotomy of planetary materials with new evidence

E. Siciliano Rego[1#*], N. Dauphas[1,2], T. Hopp[3]

https://doi.org/10.7185/geochemlet.2538

Abstract

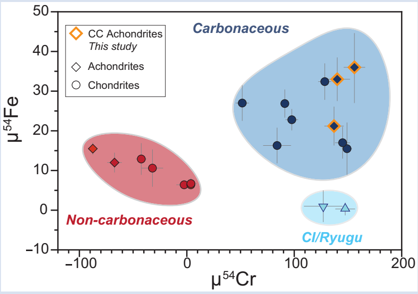

Nucleosynthetic isotope anomalies in planetary materials reveal three reservoirs in the protoplanetary disk: one in the inner Solar System, represented by non-carbonaceous chondrites (NC), and two in the outer Solar System, represented by Ivuna-type carbonaceous chondrites (CI) and other carbonaceous chondrites (CC). Separation of the CC and CI reservoirs has been debated, with some suggesting that certain carbonaceous achondrites might bridge the isotopic gap between these two groups. Our new Fe isotope data for NC and CC achondrites together with so far uncharacterised chondrite groups show that, while three ungrouped CC achondrites share O, Ti and Cr isotopic similarities with CI chondrites, their Fe isotopic compositions differ, spanning the range observed in CC meteorites. These findings reaffirm the existence of a distinct isotopic reservoir represented by CI chondrites, supporting their formation in a distinct region of the protoplanetary disk or alteration of the constituents of CC and CI parent bodies by nebular processes. The absence of CI-like differentiated bodies could be due to their parent bodies incorporating ice during formation, which limited heating.

Received 4 June 2025 | Accepted 29 August 2025 | Published 2 October 2025

Introduction

Nucleosynthetic anomalies are defined as variations in isotopic ratios that depart from mass-dependent fractionation and cannot be explained by radioactive decay or nucleogenic/cosmogenic reactions (Dauphas and Schauble, 2016). Such isotopic anomalies, commonly found in meteorites, have offered fundamental insights into material transport and mixing processes in the early Solar System. They help reveal genetic links between planets and their building blocks and delineate the regions of the protoplanetary disk from which these materials originated (Warren, 2011; Kruijer *et al.*, 2017; Dauphas *et al.*, 2024). Trinquier *et al.* (2007) first showed that non-carbonaceous (NC) and carbonaceous (CC) chondrite groups had distinct O–Cr isotopic anomalies. Warren (2011) demonstrated that this dichotomy spanned several isotopic systems and all meteorite groups. Kruijer *et al.* (2017) later revealed that the NC/CC dichotomy extended to iron meteorites, which formed earlier than chondrites, implying that the two reservoirs were spatially separated from the beginning. Ivuna-type (CI) carbonaceous chondrites define an endmember within the broader carbonaceous chondrite (CC) group in Ti–Cr isotopic space. However, the Fe isotopic compositions of CIs fall within the range of NCs, not CCs (Schiller *et al.*, 2020; Hopp *et al.*, 2022; Gattacceca *et al.*, 2025).

Hopp *et al.* (2022) studied the Fe isotopic compositions of carbonaceous chondrites and samples from the Cb-type asteroid Ryugu, which were returned to Earth by JAXA's Hayabusa2 mission (Yokoyama *et al.*, 2022). They found that CI and Ryugu exhibit distinct isotopic signatures, separate from both CC and NC. This finding was confirmed through statistical analysis of other isotopic systems (Dauphas *et al.*, 2024; Shollenberger *et al.*, 2025). Similarly, the study of the Ni isotopic composition of Ryugu and meteorites revealed that CI chondrites are distinct from other carbonaceous chondrites in their Ni isotopic anomalies (Spitzer *et al.*, 2024). This isotopic trichotomy could either reflect the existence of a third isotopic reservoir located in the outer region of the planetary accretion zone (Hopp *et al.*, 2022), or the temporal evolution of the CC reservoir through fractionation of isotopically anomalous Fe–Ni grains (Spitzer *et al.*, 2024).

Yap and Tissot (2023) argued that CI chondrites lie on extrapolated correlations of Fe, Cr and Ti isotopic anomalies in CC meteorites, implying that CI chondrites would have formed within the CC reservoir. They predicted that some carbonaceous primitive achondrite meteorites would bridge the isotopic gap between CI and CC, as these achondrites exhibit μ^{50}Ti and μ^{54}Cr isotopic anomalies approaching those observed in CI chondrites (Fig. 1). Marrocchi *et al.* (2023) supported this observation by correlating mass-dependent fractionation of Te isotopes with nucleosynthetic Fe isotope anomalies. To evaluate

1. Origins Laboratory, Department of the Geophysical Sciences and Enrico Fermi Institute, The University of Chicago, Chicago, IL 60637, USA
2. Department of Earth and Planetary Sciences, The University of Hong Kong, Hong Kong, China
3. Max-Planck-Institut für Sonnensystemforschung, 37077 Göttingen, Germany
Current address: Scripps Institution of Oceanography, Geosciences Research Division, UC San Diego, CA 92093, USA
* Corresponding author (email: erego@ucsd.edu)

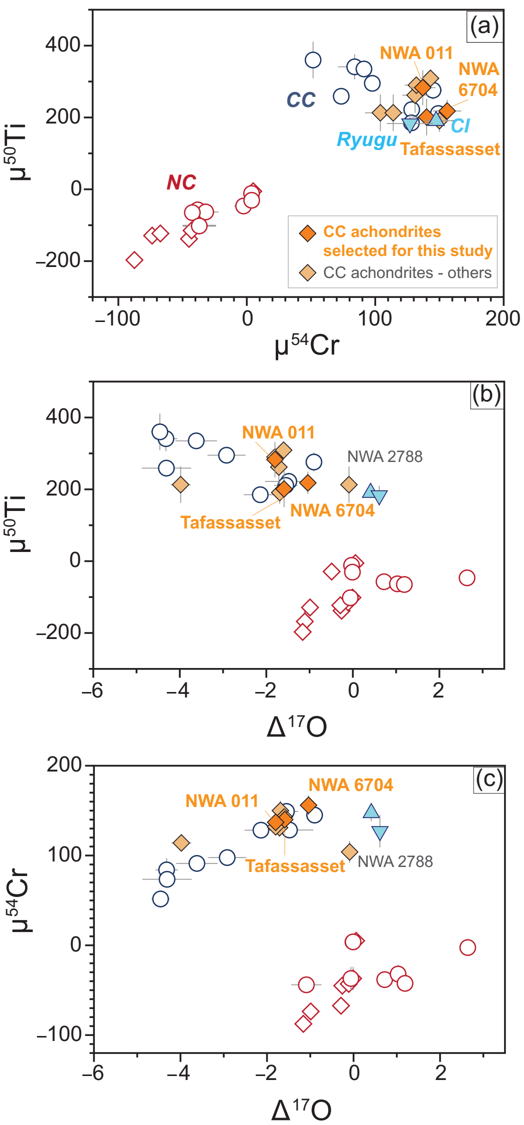

Figure 1 Plots of μ^{50}Ti *vs.* μ^{54}Cr **(a)**, μ^{50}Ti *vs.* Δ^{17}O **(b)**, and μ^{54}Cr *vs.* Δ^{17}O **(c)** for NC (open red circles for chondrites and diamonds for achondrites), non-CI carbonaceous chondrites (open dark blue circles), Ryugu/CI (light blue triangles), CC achondrites analysed in this study (dark orange diamonds) and other CC achondrites (light orange diamonds). The average Ti, Cr and O isotopic compositions of non-carbonaceous (NC) and carbonaceous (CC) meteorite groups are from the data compilation by Dauphas *et al.* (2024). Data for CC achondrites are from Yamaguchi *et al.* (2002), Trinquier *et al.* (2009), Gardner-Vandy *et al.* (2012), Göpel *et al.* (2015), Hibiya *et al.* (2019), and Williams *et al.* (2020).

the idea put forward by Yap and Tissot (2023), we present Fe isotopic data for NC and CC achondrites, as well as previously unstudied chondrite groups. Our results reveal that CC achondrites exhibit μ^{54}Fe anomalies within the same range as those observed in CC chondrites. These findings refute previous claims that CC achondrites bridge the CI–CC gap and corroborate the existence of a distinct isotopic reservoir for CI chondrites.

Results

The samples analysed in this study include three carbonaceous achondrites—Northwest Africa (NWA) 011 and NWA 6704 (both ungrouped achondrites) and Tafassasset (CR6), along with other CC and NC chondrites, including Coolidge (CL), Bencubbin (CB), Renazzo (CR), Erg Chech 002 (andesitic achondrite) and NWA 5400 (ungrouped achondrite). The iron isotopic data are reported in Tables 1 and S-1. Achondrites and carbonaceous chondrites have small mass-dependent fractionation with δ^{56}Fe values relative to reference material IRMM524A, ranging from -0.11 ± 0.02 to $+0.07 \pm 0.02$ ‰. Primitive carbonaceous achondrites NWA 011, NWA 6704 and Tafassasset show mass-independent variations with $\mu^{54}\text{Fe} = +21 \pm 5$, $+36 \pm 11$, and $+33 \pm 6$, respectively. These values are within the same range as was previously measured for CC groups CM, CO, CV, CK, CR and CH (Schiller *et al.*, 2020; Hopp *et al.*, 2022). One sample from the CR group, Renazzo (CR2), shows a CC-like μ^{54}Fe value of $+33 \pm 8$. All CRs measured in this study, including Tafassasset (CR6), have μ^{54}Fe values consistent with those of previously reported CR chondrites (Hopp *et al.*, 2022). Similarly, Bencubbin (CBa) exhibits a μ^{54}Fe value of $+36 \pm 6$, supporting a genetic link between CR, CB and CH chondrites (Weisberg *et al.*, 1995). We also analysed the iron isotopic composition of meteorite groups that had not previously been measured, including Coolidge (CL), which yield μ^{54}Fe values of $+20 \pm 8$. The iron isotopic composition of the oldest andesitic achondrite, Erg Chech 002 (Barrat *et al.*, 2021), is $\mu^{54}\text{Fe} = +10 \pm 6$, while the Brachinite-like ungrouped achondrite NWA 5400 has $\mu^{54}\text{Fe} = +9 \pm 8$.

Discussion

Hierarchical cluster analysis of meteoritic isotope data. To uncover underlying patterns in the Cr–Ti–Fe isotopic space, we use hierarchical cluster analysis (HCA), implemented with Ward's minimum variance method as the linkage criterion (see Supplementary Information). This approach groups samples based on their pairwise similarity, minimising within-cluster variance at each step. The number of clusters is not set beforehand in this approach but is decided afterward based on an

Table 1 Iron isotopic composition of primitive CC achondrites, carbonaceous chondrites and non-carbonaceous achondrites analysed in this study. Uncertainties are reported as 95 % confidence intervals.

Sample		N	μ^{54}Fe (7/6)	±	δ^{56}Fe (‰)	±
NWA 6704	CC Achondrite	14	36	11	0.01	0.02
NWA 011	CC Achondrite	12	21	5	0.03	0.03
Tafassasset	CC Achondrite	15	33	6	−0.06	0.02
Coolidge	CL	15	20	8	−0.04	0.02
Bencubbin	CB	15	36	6	−0.11	0.02
Renazzo	CR	15	33	8	0.01	0.02
Erg Chech 002	NC achondrite	15	10	6	0.07	0.02
NWA 5400	Achondrite ung.	13	9	8	−0.02	0.03

evaluation of the clustering structure. Instead of applying this approach to all isotopic anomalies (Dauphas *et al.*, 2024), focusing only on the Cr–Ti–Fe isotopic space allows us to cover a larger number of meteorites for which we have a complete dataset (Shollenberger *et al.*, 2025). This also enables us to statistically evaluate clustering in spaces where the notions of dichotomy or trichotomy have been disputed (Hopp *et al.*, 2022; Yap and Tissot, 2023).

Our statistical analysis encompasses the major meteorite groups, including CI/Ryugu, CM, CO, CV, CK, CR, CH, CB, CL, H, L, LL, R, EH, EL, HED, Ureilite, IIAB, IIIAB, IVA and CC achondrites. We normalised the isotopic anomalies for Fe, Cr and Ti using Z-score normalisation, and performed HCA using Ward's method. Hierarchical clustering using Ward's method starts with each object as its own cluster and progressively merges clusters until a single cluster remains. At each step, the Euclidean distance between cluster centroids is calculated, and the pair of clusters that produces the smallest increase in variance is merged. This produces a hierarchical structure of groupings across scales. Although HCA produces this hierarchy, it does not define the final number of clusters. To determine the optimal number of clusters in the dataset, we applied the elbow method. This method involves plotting the within-cluster sum of squares (WCSS), which is the sum of squared Euclidean distances between each point and the centroid of its assigned cluster, against the number of clusters (k). The optimal number of clusters corresponds to the inflexion point (the "elbow") in the WCSS curve, where adding further clusters results in only marginal reductions in the WCSS. We conducted this analysis using Fe, Cr and Ti isotopic systems. We identified an elbow at $k = 3$, suggesting that three clusters best capture the structure of the data (Fig. S-1). These clusters correspond to NC meteorites, CC meteorites and CI/Ryugu (Fig. 2a,b). Because neither Ward's clustering nor the elbow method account for the uncertainties in group compositions, we assessed the robustness of the clustering results using Monte Carlo simulations (MCS). These simulations involved allowing each meteorite group composition to vary according to a normal distribution, with standard deviation set by its reported uncertainty. We re-ran the clustering algorithm for each realisation and determined the optimal number of clusters using the elbow method. The elbow method consistently points to three as the optimal number of clusters (Fig. S-1). Across simulations, CI and Ryugu samples co-clustered in ~100 % of simulations, NC samples in ~100 % and CC samples in ~76 % (see SI). This analysis demonstrates that both the three-cluster solution and group assignments are robust, despite compositional uncertainties.

Persistence of the NC–CC–CI trichotomy. Previous work on the NC–CC dichotomy has shown that planetesimals formed in the inner and outer Solar System carry distinct isotopic fingerprints (Warren, 2011; Kruijer *et al.*, 2017). The possible existence of a third formation region (isotopic reservoir) for planetesimals, not sampled by NC and CC groups, was proposed by Hopp *et al.* (2022) based on high precision Fe isotopic analyses of samples from the Cb-type asteroid Ryugu. Using principal component analysis to examine isotopic anomalies in chondrites, Dauphas *et al.* (2024) found that the first principal component separated meteorites into NC and CC groups, while the second principal component isolated CI chondrites. Shollenberger *et al.* (2025) conducted a similar analysis but restricted the elements considered to Ca, Ti, Cr, Fe, Ni and Zn, as well as chemical compositions, allowing them to consider more meteorite groups. They also concluded that three distinct isotopic endmembers existed in the solar nebula. Recent Ni isotopic measurements have further confirmed that CI chondrites possess distinct isotopic compositions compared to CC chondrites (Spitzer *et al.*, 2024). Yap and Tissot (2023) challenged this view by hypothesising that Fe isotopic anomalies measured in CC achondrites would bridge the gap between Ryugu/CI and CC chondrites. The authors argued that a trend exists in the Ti–Cr–O isotopic space, extending from Ryugu/CI to other CC chondrites, indicating that these meteorites originated from a single reservoir (Marrocchi *et al.*, 2023; Yap and Tissot, 2023) (Fig. 1). By assuming that Ryugu/CI belong to the CC reservoir, Yap and Tissot (2023) conducted linear regressions through Ryugu, CI chondrites and CC chondrites in both the Fe–Cr and Fe–Ti isotopic spaces, and predicted mean μ^{54}Fe values for CC achondrites of $+14.2 \pm 4.3$ (2SE) and $+13.1 \pm 7.1$ (2SE), respectively. The authors argue that there is no need to invoke an additional reservoir to explain the large scale isotopic architecture of the early Solar System, as CC achondrites are likely to fill the isotopic gap between Ryugu/CI and CC chondrites. The CC achondrites NWA 6704/6926/6693, NWA 011 and Tafassasset were suggested candidates to bridge this isotopic gap because they only show slight

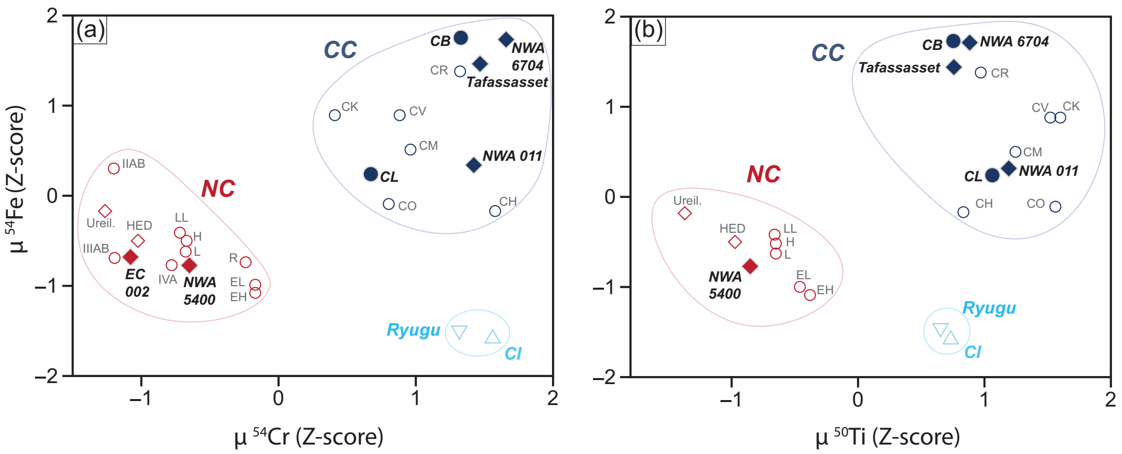

Figure 2 Hierarchical cluster analysis (HCA) of meteorite groups based on **(a)** μ^{54}Fe *vs.* μ^{54}Cr and **(b)** μ^{54}Fe *vs.* μ^{50}Ti (see main text for details and references). Isotopic values are plotted as Z-scores to normalise the differing ranges of variation and to enable consistent distance metrics for clustering. HCA was performed using Ward's method. Included groups are CI/Ryugu, CM, CO, CV, CK, CR, CH, CB, CL, H, L, LL, R, EH, EL, HED, Ureilite, IIAB, IIIAB and IVA, as well as Erg Chech 002 (EC 002), NWA 5400 and the CC achondrites analysed in this study. Samples measured in this study are shown in bold, and literature data are shown with empty symbols.

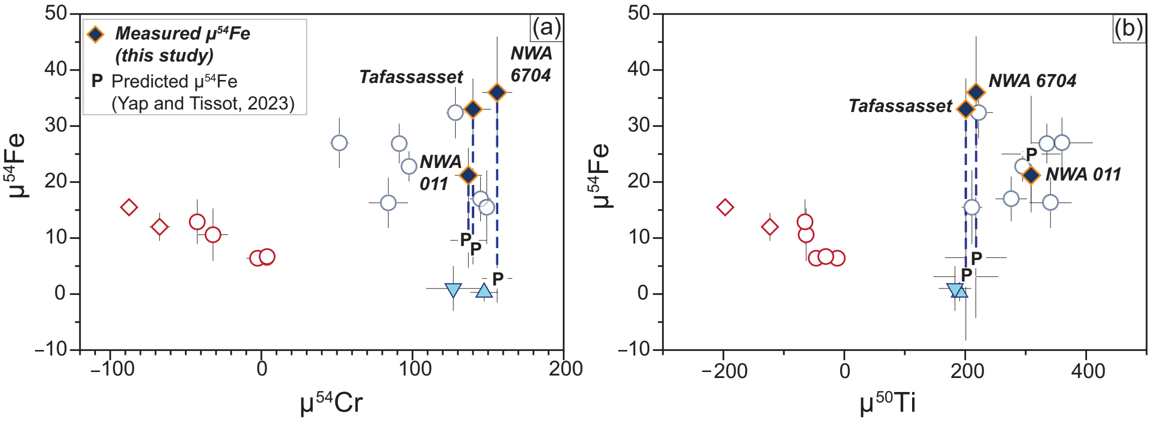

Figure 3 Plots of **(a)** μ^{54}Fe *vs.* μ^{54}Cr and **(b)** μ^{54}Fe *vs.* μ^{50}Ti, showing carbonaceous achondrites measured in this study (orange and blue diamonds), including Tafassasset, NWA 6704 and NWA 011, compared to predicted isotopic compositions (P). Dashed lines connect measured and predicted values. Diamond symbols indicate achondrites, while circles indicate chondrites. Red open symbols represent NC meteorites, blue open symbols represent CC meteorites, and filled blue symbols represent Ryugu and CI. Yap and Tissot (2023) predicted that some CC achondrites would exhibit μ^{54}Fe values intermediate between CC and CI. However, our new data show that these achondrites have μ^{54}Fe values consistent with other CC meteorites, reaffirming the isotopic trichotomy among meteorite groups.

deviations from the CI isotopic composition in Ti–Cr isotope space (Fig. 1a), with μ^{50}Ti ranging from $+201 \pm 54$ to $+283 \pm 19$ (Trinquier *et al.*, 2009; Hibiya *et al.*, 2019; Sanborn *et al.*, 2019; Williams *et al.*, 2020) and μ^{54}Cr ranging from $+137 \pm 9$ to $+156 \pm 10$ (Göpel *et al.*, 2015; Sanborn *et al.*, 2019; Williams *et al.*, 2020), while CI have μ^{50}Ti and μ^{54}Cr values of $+189 \pm 15$ and $+155 \pm 7$, respectively (Shukolyukov and Lugmair, 2006; Trinquier *et al.*, 2007, 2009; Williams *et al.*, 2020). Given the importance of this question's bearing on material transport and planetary genetics, we have decided to test the hypothesis formulated by Yap and Tissot (2023), that some CC achondrites would fill the isotopic gap between CC and CI.

Our results reveal that the Fe isotopic compositions of CC achondrites (NWA 6704, NWA 011 and Tafassasset) have μ^{54}Fe values ranging from $+21 \pm 5$ to $+36 \pm 11$. Our measured Fe isotopic compositions of CC achondrites fall within the same range as that previously measured for CC chondrites and are clearly distinct from CI (Schiller *et al.*, 2020; Hopp *et al.*, 2022) (Figs. 2,3). Thus, contrary to the predictions of Yap and Tissot (2023), the new Fe isotopic analyses of CC achondrites clearly anchor them in the CC reservoir (Fig. 3a,b), reaffirming the existence of a trichotomy in isotopic anomalies between NC, CC and CI (Hopp *et al.*, 2022).

The reason why CI chondrites stand apart from CC chondrites remains uncertain. One possibility is that, relative to CC, CI chondrites formed farther out in the protoplanetary disk, in the same region as Oort cloud comets, and were then implanted into the main asteroid belt after being dynamically excited by Uranus and Neptune (Hopp *et al.*, 2022; Nesvorný *et al.*, 2024). Such implantation requires the presence of nebular gas to dampen eccentricities. In this context, the absence of isotopic anomalies intermediate between CC and CI could be explained by the dynamics of planetesimals in the region between the gas and ice giant planets. These planetesimals could have had isotopic compositions intermediate between CC and CI, as suggested by Yap and Tissot (2023), but they were dynamically excited by giant planets after the dissipation of nebular gas, hindering their implantation into the main asteroid belt. An alternative explanation is that CC and CI chondrites formed in the same reservoir but at a different time or by different processes, leading to their distinct isotopic signatures. Recently, Spitzer *et al.* (2024) proposed that the accretion of CI chondrite parent bodies was triggered by photoevaporation at the end of the disk lifetime, and incorporated a higher fraction of hypothetical Fe–Ni metal alloy with exotic isotopic composition (Spitzer *et al.*, 2024).

As shown here, achondrites associated with carbonaceous meteorites have isotopic anomalies that are distinctly different from those of CI chondrites (Fig. 3). While it is likely that we have not yet accessed the full inventory of Solar System materials, the CI-like isotopic signature has, to date, only been observed in primitive objects that appear to have escaped ^{26}Al-induced melting. The absence of differentiated CI bodies could be explained by late formation of CI parent bodies preventing production of enough heat by decay of ^{26}Al required for differentiation (Spitzer *et al.*, 2024). However, whether CI chondrite/Ryugu parent bodies accreted late is still debated (McCain *et al.*, 2023; Tanaka *et al.*, 2024). Hopp *et al.* (2022) and Nesvorný *et al.* (2024) proposed that CI chondrites likely formed in the same region of the protoplanetary disk as Oort cloud comets, meaning that they would have accreted significant amounts of ice. Others have also proposed a genetic link between CI chondrites and comets (Gounelle, 2011). The fact that CI parent bodies avoided heating and differentiation may be attributed to the presence of water ice in the parent body. Indeed, simulations of the thermal evolution of ice-bearing planetesimals (Grimm and Mcsween, 1989; Wakita and Sekiya, 2011) have demonstrated that heating in such bodies is limited by several factors: (i) the melting of ice, which absorbs significant amounts of radioactive heat as latent heat; and (ii) hydrothermal circulation, which transports heat from the interior to the surface, where it is radiated away. Additionally, under low lithostatic pressure, processes such as ice sublimation and liquid water vaporisation can also absorb substantial heat. These mechanisms may account for the absence of differentiated objects within the CI-clan (Hopp *et al.*, 2022; Dauphas *et al.*, 2024), as such objects likely formed further out in the disk and possessed a higher ice-to-rock ratio compared to CC meteorites (Hopp *et al.* 2022; Nesvorný *et al.*, 2024).

Acknowledgements

We thank the Field Museum for providing samples used in this study. Constructive criticism from three anonymous reviewers and editors was greatly appreciated. This work was supported by NASA grants 80NSSC23K1022 (LARS), 80NSSC21K0380 and 80NSSC20K0821 (Emerging Worlds), 80NSSC23K1163 (MMX-PSP), and DOE grant DE-SC0022451 to N.D.

Editor: Romain Tartèse

Additional Information

Supplementary Information accompanies this letter at https://www.geochemicalperspectivesletters.org/article2538.

Cite this letter as: Siciliano Rego, E., Dauphas, N., Hopp, T. (2025) Consolidating the isotopic trichotomy of planetary materials with new evidence. *Geochem. Persp. Let.* 37, 7–11. https://doi.org/10.7185/geochemlet.2538

References

Barrat, J.A., Chaussidon, M., Yamaguchi, A., Beck, P., Villeneuve, J., Byrne, D.J., Broadley, M.W., Marty, B. (2021) A 4,565-My-old andesite from an extinct chondritic protoplanet. *Proceedings of the National Academy of Sciences of the United States of America* 118, 1–7. https://doi.org/10.1073/pnas.2026129118

Dauphas, N., Schauble, E.A. (2016) Mass Fractionation Laws, Mass-Independent Effects, and Isotopic Anomalies. *Annual Review of Earth and Planetary Sciences* 44, 709–783. https://doi.org/10.1146/annurev-earth-060115-012157

Dauphas, N., Hopp, T., Nesvorný, D. (2024) Bayesian inference on the isotopic building blocks of Mars and Earth. *Icarus* 408, 115805. https://doi.org/10.1016/j.icarus.2023.115805

Gardner-Vandy, K.G., Lauretta, D.S., Greenwood, R.C., McCoy, T.J., Killgore, M., Franchi, I.A. (2012) The Tafassasset primitive achondrite: Insights into initial stages of planetary differentiation. *Geochimica et Cosmochimica Acta* 85, 142–159. https://doi.org/10.1016/j.gca.2012.01.014

Gattacceca, J., Gounelle, M., Devouard, B., Barrat, J.-A., Bonal, A., *et al.* (2025) Oued Chebeika 002: A new CI1 meteorite linked to outer solar system bodies. *Meteoritics and Planetary Science* 60, 1441–1479. https://doi.org/10.1111/maps.14359

Göpel, C., Birck, J.L., Galy, A., Barrat, J.A., Zanda, B. (2015) Mn-Cr systematics in primitive meteorites: Insights from mineral separation and partial dissolution. *Geochimica et Cosmochimica Acta* 156, 1–24. https://doi.org/10.1016/j.gca.2015.02.008

Gounelle, M. (2011) The asteroid-comet continuum: In search of lost primitivity. *Elements* 7, 29–34. https://doi.org/10.2113/gselements.7.1.29

Grimm, R.E., Mcsween, H.Y. (1989) Water and the thermal evolution of carbonaceous chondrite parent bodies. *Icarus* 82, 244–280. https://doi.org/10.1016/0019-1035(89)90038-9

Hibiya, Y., Archer, G.J., Tanaka, R., Sanborn, M.E., Sato, Y., Iizuka, T., Ozawa, K., Walker, R.J., Yamaguchi, A., Yin, Q.-Z., Nakamura, T., Irving, A.J. (2019) The origin of the unique achondrite Northwest Africa 6704: Constraints from petrology, chemistry and Re–Os, O and Ti isotope systematics. *Geochimica et Cosmochimica Acta* 245, 597–627. https://doi.org/10.1016/j.gca.2018.04.031

Hopp, T., Dauphas, N., Abe, Y., Aléon, J., Alexander, C.M.O'D. *et al.* (2022) Ryugu's nucleosynthetic heritage from the outskirts of the Solar System. *Science Advances* 8, 1–10. https://doi.org/10.1126/sciadv.add8141

Kruijer, T.S., Burkhardt, C., Budde, G., Kleine, T. (2017) Age of Jupiter inferred from the distinct genetics and formation times of meteorites. *Proceedings of the National Academy of Sciences of the United States of America* 114, 6712–6716. https://doi.org/10.1073/pnas.1704461114

Marrocchi, Y., Piralla, M., Tissot, F.L.H. (2023) Iron Isotope Constraints on the Structure of the Early Solar System. *The Astrophysical Journal Letters* 954, L27. https://doi.org/10.3847/2041-8213/acefd1

McCain, K.A., Matsuda, M., Liu, M.-C., McKeegan, K.D., Yamaguchi, A., *et al.* (2023) Early fluid activity on Ryugu inferred by isotopic analyses of carbonates and magnetite. *Nature Astronomy* 7, 309–317. https://doi.org/10.1038/s41550-022-01863-0

Nesvorný, D., Dauphas, N., Vokrouhlický, D., Deienno, R., Hopp, T. (2024) Isotopic trichotomy of main belt asteroids from implantation of outer solar system planetesimals. *Earth and Planetary Science Letters* 626, 118521. https://doi.org/10.1016/j.epsl.2023.118521

Sanborn, M.E., Wimpenny, J., Williams, C.D., Yamakawa, A., Amelin, Y., Irving, A.J., Yin, Q.Z. (2019) Carbonaceous achondrites Northwest Africa 6704/6693: Milestones for early Solar System chronology and genealogy. *Geochimica et Cosmochimica Acta* 245, 577–596. https://doi.org/10.1016/j.gca.2018.10.004

Schiller, M., Bizzarro, M., Siebert, J. (2020) Iron isotope evidence for very rapid accretion and differentiation of the proto-Earth. *Science Advances* 6, 1–7. https://doi.org/10.1126/sciadv.aay7604

Shollenberger, Q.R., Render, J., Wimpenny, J., Armytage, R.M.G., Gunawardena, N., Rolison, J.M., Simon, J.I., Brennecka, G.A. (2025) Elemental and isotopic signatures of Asteroid Ryugu support three early Solar System reservoirs. *Earth and Planetary Science Letters* 664, 119443. https://doi.org/10.1016/j.epsl.2025.119443

Shukolyukov, A., Lugmair, G.W. (2006) Manganese-chromium isotope systematics of carbonaceous chondrites. *Earth and Planetary Science Letters* 250, 200–213. https://doi.org/10.1016/j.epsl.2006.07.036

Spitzer, F., Kleine, T., Burkhardt, C., Hopp, T., Yokoyama, T., *et al.* (2024) The Ni isotope composition of Ryugu reveals a common accretion region for carbonaceous chondrites. *Science Advances* 10, eadp2426. https://doi.org/10.1126/sciadv.adp2426

Tanaka, R., Ratnayake, D.M., Ota, T., Miklusicak, N., Kunihiro, T., *et al.* (2024) Unraveling the Cr Isotopes of Ryugu: An Accurate Aqueous Alteration Age and the Least Thermally Processed Solar System Material. *The Astrophysical Journal* 965, 52. https://doi.org/10.3847/1538-4357/ad276a

Trinquier, A., Birck, J., Allegre, C.J. (2007) Widespread 54 Cr Heterogeneity in the Inner Solar System. *The Astrophysical Journal* 655, 1179–1185. https://doi.org/10.1086/510360

Trinquier, A., Elliott, T., Ulfbeck, D., Coath, C., Krot, A.N., Bizzarro, M. (2009) Origin of Nucleosynthetic Isotope Heterogeneity in the Solar Protoplanetary Disk. *Science* 324, 374–376. https://doi.org/10.1126/science.1168221

Wakita, S., Sekiya, M. (2011) Thermal evolution of icy planetesimals in the solar nebula. *Earth, Planets and Space* 63, 1193–1206. https://doi.org/10.5047/eps.2011.08.012

Warren, P.H. (2011) Stable-isotopic anomalies and the accretionary assemblage of the Earth and Mars: A subordinate role for carbonaceous chondrites. *Earth and Planetary Science Letters* 311, 93–100. https://doi.org/10.1016/j.epsl.2011.08.047

Weisberg M.K., Prinz, M., Clayton, R.N., Mayeda, T.K., Grady, M.M., Pillinger, C.T. (1995) The CR chondrite clan. *Proceedings of the NIPR Symposium on Antarctic Meteorites* 8, 11–32.

Williams, C.D., Sanborn, M.E., Defouilloy, C., Yin, Q.Z., Kita, N.T., Ebel, D.S., Yamakawa, A., Yamashita, K. (2020) Chondrules reveal large-scale outward transport of inner Solar System materials in the protoplanetary disk. *Proceedings of the National Academy of Sciences of the United States of America* 117, 23426–23435. https://doi.org/10.1073/pnas.2005235117

Yamaguchi, A., Clayton, R.N., Mayeda, T.K., Ebihara, M., Oura, Y., *et al.* (2002) A new source of basaltic meteorites inferred from Northwest Africa 011. *Science* 296, 334–336. https://doi.org/10.1126/science.1069408

Yap, T.E., Tissot, F.L.H. (2023) The NC-CC dichotomy explained by significant addition of CAI-like dust to the Bulk Molecular Cloud (BMC) composition. *Icarus* 405, 115680.https://doi.org/10.1016/j.icarus.2023.115680

Yokoyama, T., Nagashima, K., Nakai, I., Young, E.D., Abe, Y., *et al.* (2022) Samples returned from the asteroid Ryugu are similar to Ivuna-type carbonaceous meteorites. *Science* 379, 1–10. https://doi.org/10.1126/science.abn7850